This article was downloaded by: [Xian Jiaotong University]
On: 11 December 2014, At: 13:22
Publisher: Taylor & Francis
Informa Ltd Registered in England and Wales Registered Number: 1072954 Registered office: Mortimer House, 37-41 Mortimer Street, London W1T 3JH, UK

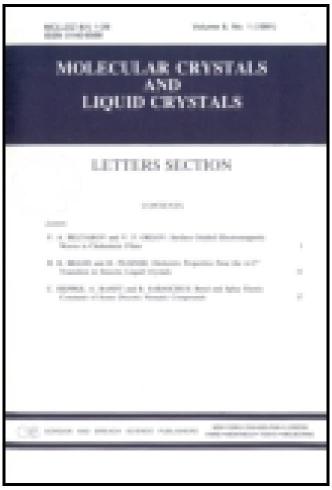

Molecular Crystals and Liquid Crystals
Publication details, including instructions for authors and subscription information:
http://www.tandfonline.com/loi/gmcl20

The Effects of Varied Deposition Conditions, Including the Use of Argon, on Thin-Film Silicon Solar Cells Prepared using PECVD

L. J. Crudgington[a], M. A. Rind[a], D. N. R. Payne[a] & D. M. Bagnall[a]
[a] School of Electronics and Computer Science, University of Southampton, Southampton, UK

Published online: 08 Apr 2014.

To cite this article: L. J. Crudgington, M. A. Rind, D. N. R. Payne & D. M. Bagnall (2014) The Effects of Varied Deposition Conditions, Including the Use of Argon, on Thin-Film Silicon Solar Cells Prepared using PECVD, Molecular Crystals and Liquid Crystals, 591:1, 91-113, DOI: 10.1080/15421406.2013.827855

To link to this article: http://dx.doi.org/10.1080/15421406.2013.827855

PLEASE SCROLL DOWN FOR ARTICLE

Taylor & Francis makes every effort to ensure the accuracy of all the information (the "Content") contained in the publications on our platform. However, Taylor & Francis, our agents, and our licensors make no representations or warranties whatsoever as to the accuracy, completeness, or suitability for any purpose of the Content. Any opinions and views expressed in this publication are the opinions and views of the authors, and are not the views of or endorsed by Taylor & Francis. The accuracy of the Content should not be relied upon and should be independently verified with primary sources of information. Taylor and Francis shall not be liable for any losses, actions, claims, proceedings, demands, costs, expenses, damages, and other liabilities whatsoever or howsoever caused arising directly or indirectly in connection with, in relation to or arising out of the use of the Content.

This article may be used for research, teaching, and private study purposes. Any substantial or systematic reproduction, redistribution, reselling, loan, sub-licensing, systematic supply, or distribution in any form to anyone is expressly forbidden. Terms & Conditions of access and use can be found at http://www.tandfonline.com/page/terms-and-conditions

Mol. Cryst. Liq. Cryst., Vol. 591: pp. 91–113, 2014

ISSN: 1542-1406 print/1563-5287 online
DOI: 10.1080/15421406.2013.827855

The Effects of Varied Deposition Conditions, Including the Use of Argon, on Thin-Film Silicon Solar Cells Prepared using PECVD

L. J. CRUDGINGTON,* M. A. RIND, D. N. R. PAYNE,
AND D. M. BAGNALL

School of Electronics and Computer Science, University of Southampton,
Southampton, UK

This paper reports the effects of varied deposition conditions on the resultant energy conversion efficiencies of thin-film silicon solar cells. Cells were deposited using an Oxford Instruments PlasmaLab System 100 on to Pilkington TEC-8 TCO glass, and thoroughly investigated using electrical methods. Thin film devices were fabricated using the decomposition of silane gas within a reaction chamber of 13.56 MHz plasma discharge. The deposition conditions, including substrate temperature, gas flow rates, RF power, chamber pressure, and film thickness are all explored to determine the optimum cell performance. A view toward high-efficiency solar structures, including heterojunction with intrinsic thin layer (HIT) and micro-morph cell designs using the same conditions is presented.

Keywords Amorphous; HIT; micro-morph; PECVD

I. Introduction

PROPER understanding of the effects of the many possible deposition conditions are essential when attempts are made to improve the efficiency of a solar cell made using the PECVD technique. Amorphous hydrogenated silicon thin films are very versatile materials, allowing for effective photo-active devices to be deposited on to low-cost substrate materials such as glass or aluminum. However, despite their low-cost and ease of fabrication, amorphous silicon devices have not acquired substantial market penetration and remain with only 5% of the photovoltaic market share [1]. In order to increase competitiveness, several performance aspects of the silicon thin films must be improved upon.

This paper attempts to describe how the slight differences in the process conditions while using PECVD for deposition of amorphous silicon thin films can affect the resultant performance of the solar device. From this investigation, the starting point deposition conditions for development of a deposition process can be readily known, which will help to reduce the development time. Currently, the deposition rate of the PECVD process is low, and therefore the cost to explore the parameter space of a new process can be needlessly high.

---

*Address correspondence to L. J. Crudgington, School of Electronics and Computer Science, University of Southampton, Southampton SO17 1BJ, UK. Tel.: 023 8059 2422. E-mail: ljc1g09@ecs.soton.ac.uk

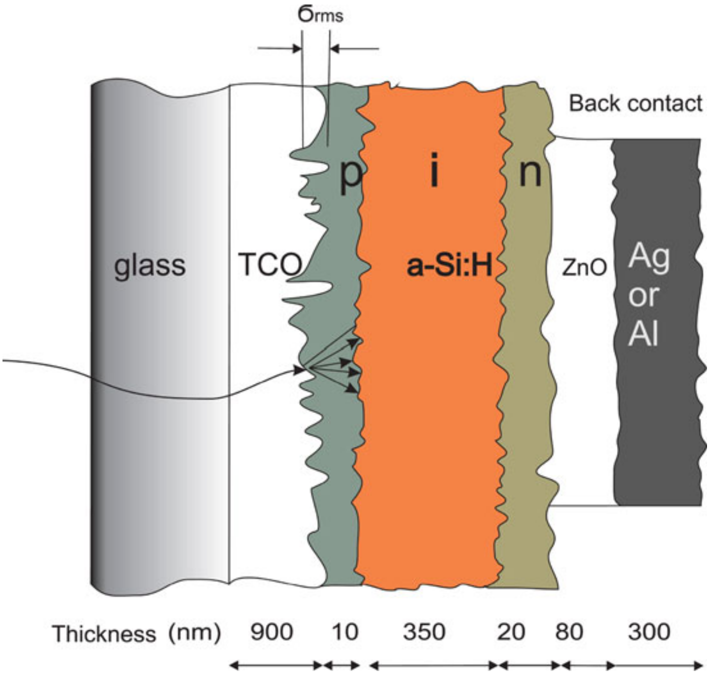

Figure 1. P-I-N structure [Reproduced from 4].

II. Amorphous Silicon Devices

Due to the extremely low carrier mobility within doped regions of hydrogenated amorphous silicon, the conventional P-N structure utilized by c-Si solar cells provides very low energy conversion efficiencies. The initial experiments were performed by Spear et al. in the mid-1970s, and illustrated that the P-N technique was possible [2]; however, the first cells developed with appreciable energy conversion efficiencies were of the P-I-N structure. This serves to provide a much larger depletion region "drift zone" for carrier collection. Carlson and Wronski [3] were able to fabricate a P-I-N structure on TCO coated glass with an aluminum back reflector, which resulted in 2% energy conversion efficiency. This type of device topology is depicted in Fig. 1.

III. Experimental Detail

In this investigation, deposition is performed using an Oxford Instruments PlasmaLab System 100. This system uses an ionized plasma glow discharge to disassociate the source gases into their elemental components and deposit on to the substrate material. RF electrodes are positioned above and below the substrate, which when active cause chemical vapor deposition to occur while the substrate is kept at much lower temperatures than would otherwise be required. The excitation frequency of this system is 13.56 MHz, which supplies ample excitation energy at low power whilst minimizing ion bombardment damage to the growing films.

The deposition chamber is supplied with source gases via a series of programmable mass-flow controllers (MFCs) which combine and provide the atomic species for CVD via a uniform shower-head arrangement. Pressure is regulated within the chamber using a programmable APC valve and a turbo/base pump combination with integrated nitrogen pump purge.

The deposition conditions for PECVD are variable, and include gas flow rates, chamber pressure, substrate temperature, RF power, and deposition time. The geometry of the deposition reactor chamber and RF electrodes also affect the performance of the reaction, and therefore the data ascertained for this experiment will only be repeatable of an identically specified system. The dilution of SiH_4 and the choice of dilute gas can also significantly influence the electrical performance. Each individual layer of the P-I-N structure must be optimized in thickness, which forms the basis of the process development routine.

TCO Glass materials are chosen to perform the deposition of amorphous silicon P-I-N structures. The TCO coating is electrically conductive and allows the front contact of the device to be free of any metallization to provide the optimum surface for thin-film silicon deposition. TEC-8 (Transparent Electrically Conductive) glass is specially selected to have the lowest series resistance within the Pilkington range, while retaining a certain amount of haze ideally suited to the deposition of amorphous silicon. The resistivity of the TEC-8 glass is approximately 6–9 Ω/sq, making for an excellent front contact [5].

It is essential to ensure that the substrate material is perfectly clean before deposition begins. Contamination of the substrate can cause many performance-reducing effects, including poor adhesion of the deposited film, and shunting due to pin-holes shorting the active region of the device. Therefore, a series of thorough sample cleaning techniques must be undertaken. Specifically, a contaminant such as a dust particle can cause a defect in the uniformity of the deposited film causing surface roughness, PECVD having nonconformal step coverage. Additionally, if the particle is removed during subsequent chamber pumping steps or substrate handling, the TCO of the substrate will become exposed. Metallization over this region will directly contact the TCO and cause a short circuit "shunt" condition. If substrates have been handled in order to dice the material into the size required, then the first step in cleaning is to use a simple degreaser such as washing-up liquid and clean the sample by hand. This has been shown to remove a significant amount of contamination and dust particles from the shipping package, and the use of latex gloves will not add any additional contamination.

The standard cleaning technique before deposition is to initially rinse the sample with de-ionized water to remove any particles that may have been picked up. The next step is to thoroughly clean the sample with acetone solvent in order to remove organic materials from the sample. After the majority of the acetone has evaporated away, the sample is thoroughly cleaned using isopropanol alcohol (IPA). A final spray with nitrogen assists the drying of the sample and removes any additional particles. It is also suggested that a nitrogen blow is performed if the samples are left in the open for any length of time.

IV. Deposition

The first step of the fabrication process is to determine the optimum deposition conditions for each layer. Initially, beginning with full P-I-N structures may lead to a quicker series of results; however, the data obtained from these results will tell very little about the internal behavior of the cell and make it difficult to diagnose poor performance or seek higher efficiencies. For these purposes, it is essential to fabricate individual thin film single layers using varying deposition conditions, and thoroughly examine their optical and electrical performance before committing these conditions to a complete P-I-N device. The first step is to examine the dark and photo conductivities (σ), optical band gap (E_g), optical absorption and reflectivity at various wavelengths and thin film thickness. From these experiments it

Table 1. Intrinsic layer deposition parameters

Variable	Unit	Value
RF power	(W)	10
Temp	(°C)	250
Chamber pressure	(mTorr)	750
SiH_4 flow rate	(sccm)	50
H_2 flow rate	(sccm)	50
I-layer deposition time	(min:sec)	25:38
Thickness	I (nm)	400

is possible to determine specific deposition problems such as inefficient doping of layers or contamination of intrinsic material.

Once optimum layer quality has been obtained, deposition of P-I-N structures using the optimized single-layer conditions is performed, and the device can be examined by means of I-V curve and quantum efficiency measurement, which can be used to determine the energy conversion efficiency (η), fill factor, V_{OC}, I_{SC}, and maximum power output. In addition, the effects of controlling the rate of reaction using a dilution of inert argon gas will be investigated, to examine the effects on the electrical properties of the resultant silicon thin films. Rear contacting of the device is performed using deposition of 500 nm Al, using e-beam assisted evaporation through a 9-region stencil mask.

A. *Intrinsic Layers*

The intrinsic region of the P-I-N structure is fundamental in defining the performance of the solar device. This region performs all of the photon absorption and conversion into charge carriers, and therefore must be highly passivated and free from all contamination which could provide Shockley-Reid-Hall recombination centers [6]; the hydrogen passivation efficiency is therefore very important in this region. While the atomic hydrogen species in the SiH_4 source gas is often sufficient, dilution in additional elemental hydrogen (H_2) will be investigated.

A series of intrinsic layers have been fabricated in order to determine the effects of the various conditions. Results are presented in the form of dark and photo conductivities (σ) presented on the same axis, which illustrates the intrinsic layer performance. A larger difference ratio between dark and photo conductivity, alongside the lowest conductivities is desirable for purely intrinsic material with no dopants or contamination [7]. Conditions not under test have been kept constant for all depositions, the values of which are presented in Table 1. These variables have been determined as a good baseline set of conditions from prior depositions.

(1) Variation of RF Power on Intrinsic Layers. The RF power can significantly affect the deposition time and electrical quality of silicon thin films. The capacitive-coupled 13.56 MHz RF generator is controllable up to a power of 200 W. Increasing the power can provide faster deposition rates but can reduce yield and repeatability; while a low RF power combined with a low chamber pressure can cause failure of the plasma to start. For these reasons, the maximum power investigated is 30 W. In this investigation, conductivity

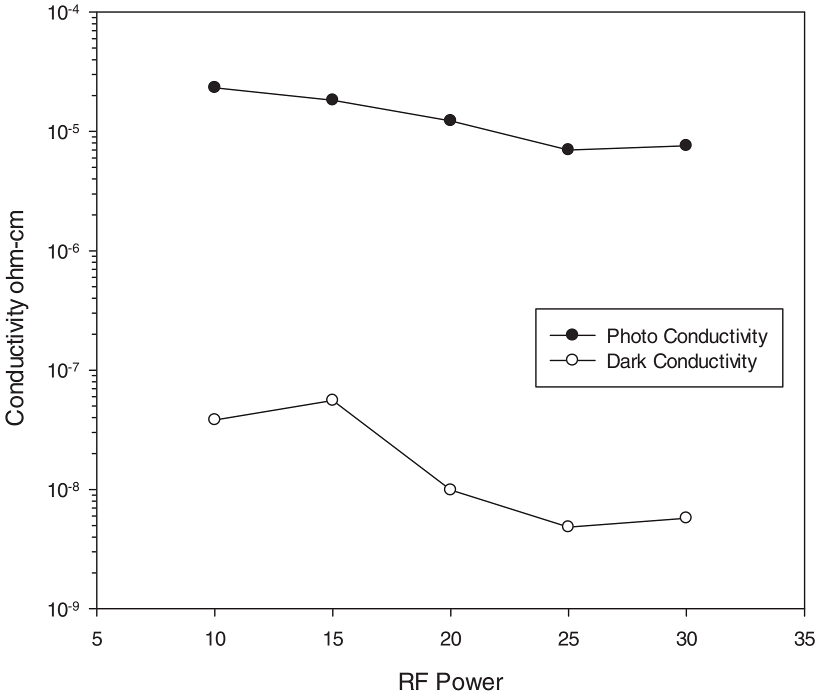

Figure 2. Conductivity vs. RF power.

parameters under dark and illuminated conditions are shown as a function of RF power varied from 10 W to 30 W in steps of 5 W shown in Fig. 2.

(2) Variation of Chamber Pressure on Intrinsic Layers. The chamber pressure can also affect the deposition time and electronic properties of silicon thin films. In addition, as suggested in Section 1 above, low chamber pressures combined with low RF power can cause intermittent failure of the plasma to ignite, for this reason 300 mT is the minimum pressure used. In this investigation, parameters are shown as a function of intrinsic layer pressure, varied from 300 mT to 500 mT in steps of 50 mT shown in Fig. 3.

(3) Variation of Temperature on Intrinsic Layers. Substrate temperature affects the speed of film formation of the surface of the substrate, and can also alter the crystallinity of the resultant film due to the application of more thermal energy to the process gases as they reach the substrate, providing more time for the adatoms to desorb across the surface and find a suitable site. The temperature of the substrate is controlled via resistive heating of the table unit fitted inside the deposition chamber. In this investigation, conductivity parameters are shown as a function of substrate temperature varied from 150°C to 350°C in steps of 50°C shown in Fig. 4.

(4) Variation of Hydrogen Dilution on Intrinsic Layers. The hydrogen content of the process gas will affect the crystallinity and deposition rate of the silicon films [8]. Polycrystalline material is undesirable as its properties differ significantly from what is desired, which an excess of hydrogen gas during deposition will provide. In this investigation, conductivity

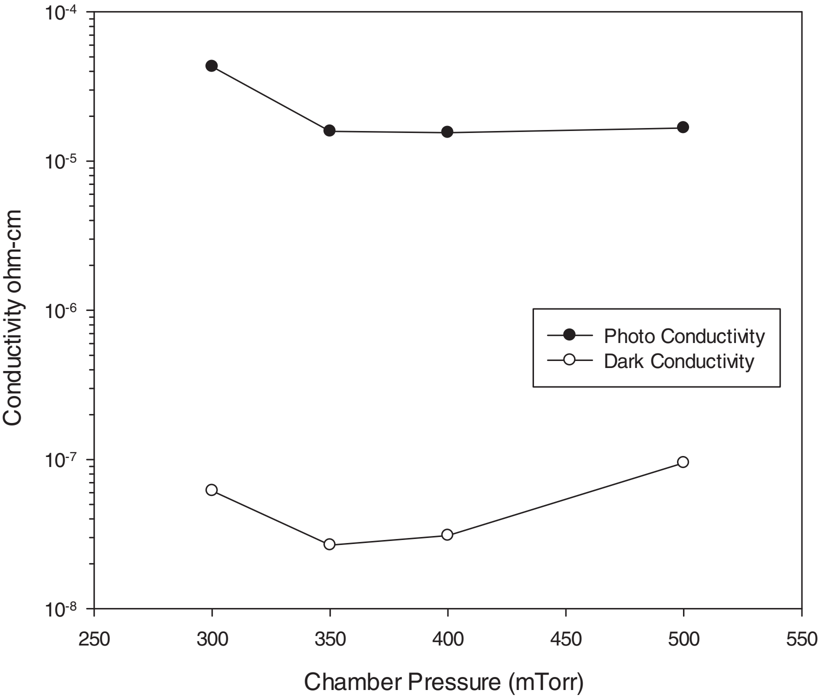

Figure 3. Conductivity vs. chamber pressure.

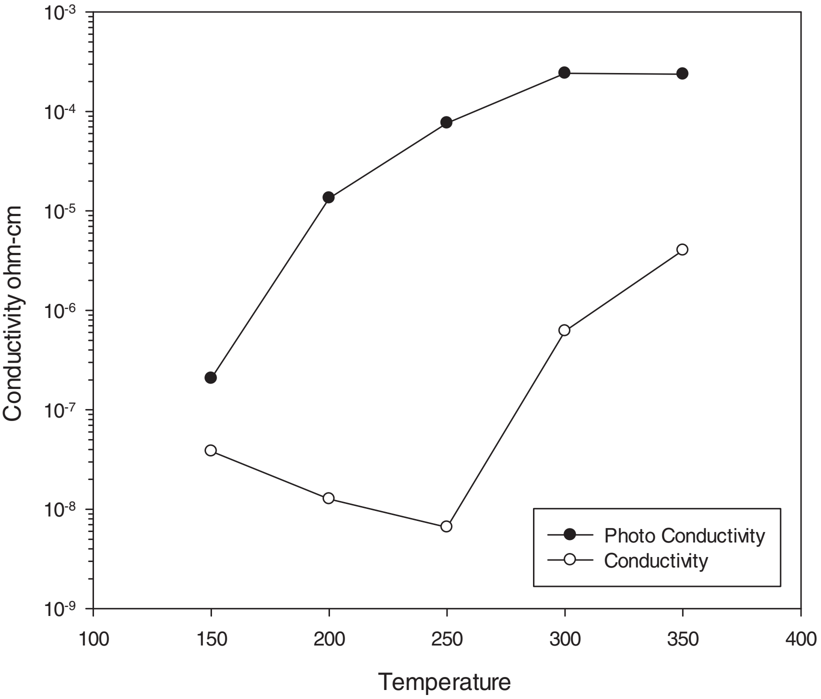

Figure 4. Conductivity vs. temperature.

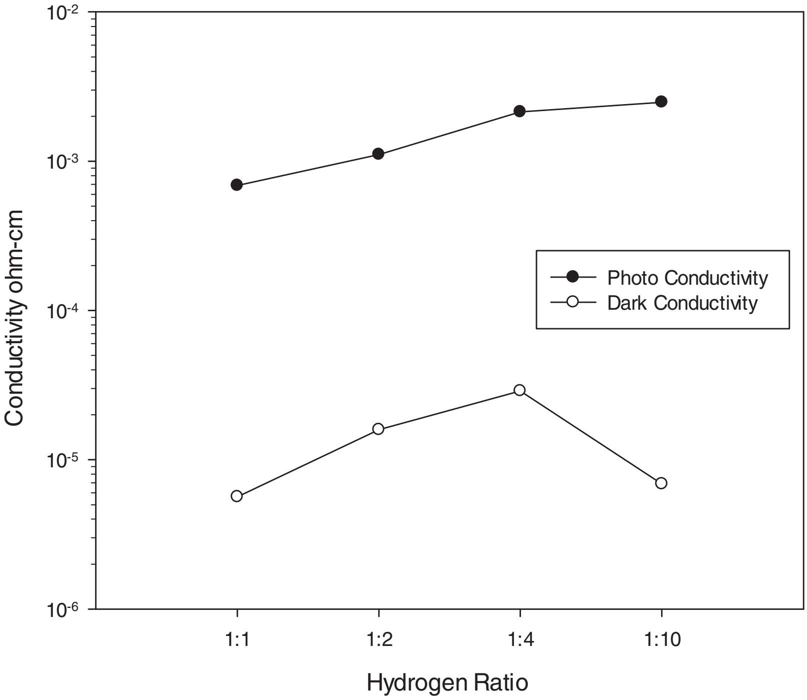

Figure 5. Conductivity vs. flow rate.

parameters under dark and illuminated conditions are shown as a function of hydrogen inclusion (1:1–1:10) shown in Fig. 5.

(5) Thickness Variation of Intrinsic Layers. The variation in thickness is determined using spectroscopic ellipsometry. Figure 6 details the ellipsometry result of a 350 nm intrinsic layer. This layer was deposited at the optimum deposition conditions as determined in this section, shown in Section V.

B. Doped Layers

In order to create a functioning P-I-N device, thin layers of doped amorphous silicon must be deposited either side of the intrinsic region. The next step in the optimization process is to determine the optimum concentration of dopant gas in the p-type and n-type regions. If the dopant gases are too dilute then the electric field generated by the layer will not be sufficient as the layer will behave as intrinsic, however, if the doping concentration is too high then the recombination losses in the region will dominate. Low concentrations are expected to illustrate intrinsic behavior similar to the films shown in Section A, and dark conductivity is quickly expected to approach photo conductivity as the dopant concentration is increased.

All conditions not under test have been kept constant and are summarized Table 2. The resultant dark and photo-conductivity measurements and the dark/photo ratios for each investigation are then presented.

The phosphine and diborane supply to the system is 10% dilute in argon gas in order to ensure safety and effective control over the doping of the devices. Due to the very low

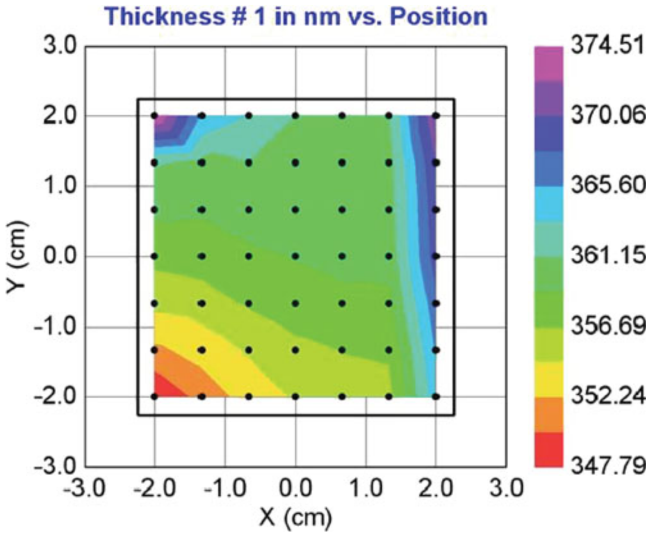

Figure 6. Thickness profile determined by ellipsometry.

flow rate of dopant gas compared to the silane and hydrogen supplies, this trace volume of argon is not thought to affect the layer performance as is shown in Section 3C.

(1) P-type Dopant Concentration. Optimization of the p-type region is vital in achieving high performance from a P-I-N device, as it is the first layer in which the incoming light encounters. This region has a very low charge carrier lifetime and therefore photons absorbed are often lost via recombination. For this reason, it should be kept extremely thin while still providing an adequate electric field over the device. In this investigation, the gas diborane (B_2H_6) is mixed with a flow of silane gas in concentrations of 0.2% to 2.4% shown in Fig. 7.

(2) N-type Dopant Concentration. Optimization of the n-type region is also significant in determining the performance of a device, as this layer is positioned immediately before the aluminum back reflector and therefore is passed twice by incoming light. For this reason, the dopant concentration should be lower to minimize recombination losses, and

Table 2. Doped layer deposition parameters

Variable	Unit	Value
RF tower	(W)	10
Temp	(°C)	250
Chamber pressure	(mTorr)	350
SiH_4 flow rate	(sccm)	50
Thickness	*P* (nm)	10
Thickness	*N* (nm)	40
Deposition rate	P-layer (nm/sec)	0.60
Deposition rate	N-layer (nm/sec)	0.26

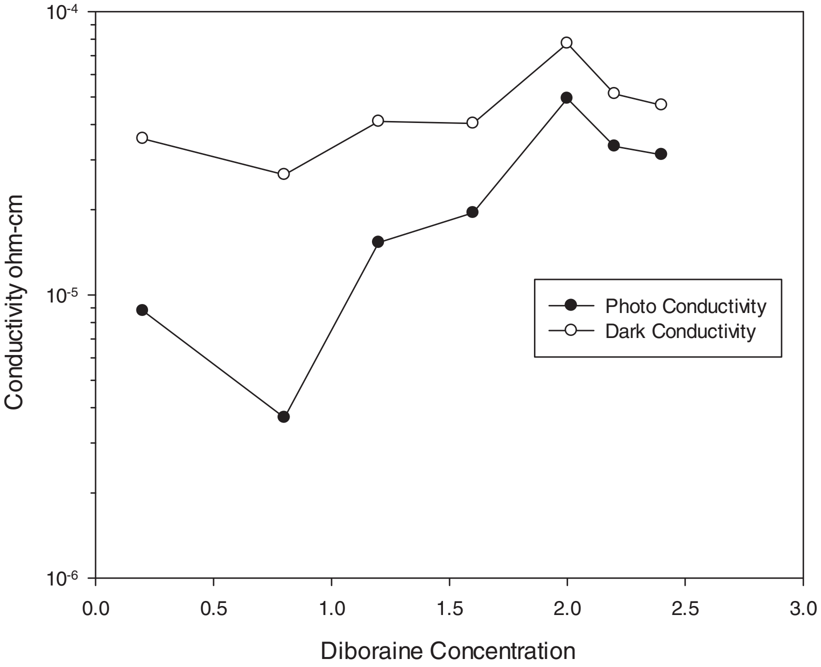

Figure 7. Conductivity vs. diboraine concentration.

therefore the thickness of the layer must be made wider to generate the corresponding electric field. In this investigation, the gas phosphine (PH_3) is mixed with a flow of silane gas in concentrations of 0.2%–2% shown in Fig. 8.

C. P-I-N Structure Devices

Based on the optimum results from the single layer investigations in Sections A and B, a series of P-I-N structures have been fabricated in order to determine the effects of variations in layer thickness. The conditions have been kept the same for all variables excluding the deposition time, which directly determines the layer thickness. The resultant energy conversion efficiencies, fill factors, V_{OC} and I_{SC} for each investigation are presented.

(1) Variation of p-Type Layer Thickness. The p-type layer thickness is fundamental in determining the performance of the photovoltaic device. For this reason, this is very sensitive to thickness variations and must be kept thin while retaining adequate electrical ability to provide charge carrier separation together with the n-type layer at the rear of the device. Parameters are shown as a function of p-layer thickness, plotted against energy conversion efficiency, fill factor, V_{OC} and I_{SC}, shown in Figs. 9 and 10, respectively. Layer thickness is varied from 8 nm to 15 nm in steps of 2–3 nm.

(2) Variation of Intrinsic Layer Thickness. The intrinsic layer thickness is additionally fundamental in determining the performance of the photovoltaic device. It is this layer in which the vast majority of photons are absorbed so the layer must exhibit exceptional intrinsic properties such as dark/photo conductivity ratio. A peak in performance will exist

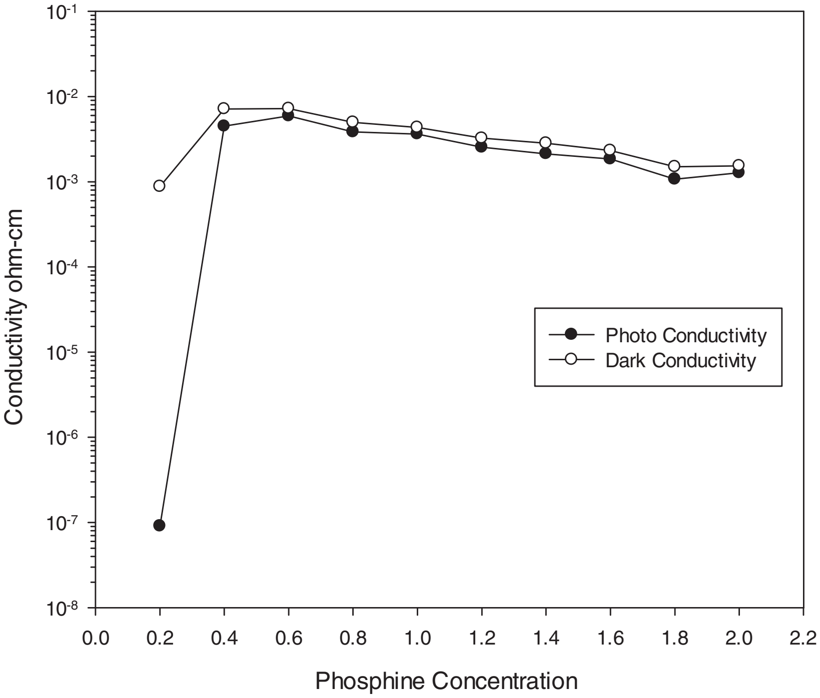

Figure 8. Conductivity vs. phosphine concentration.

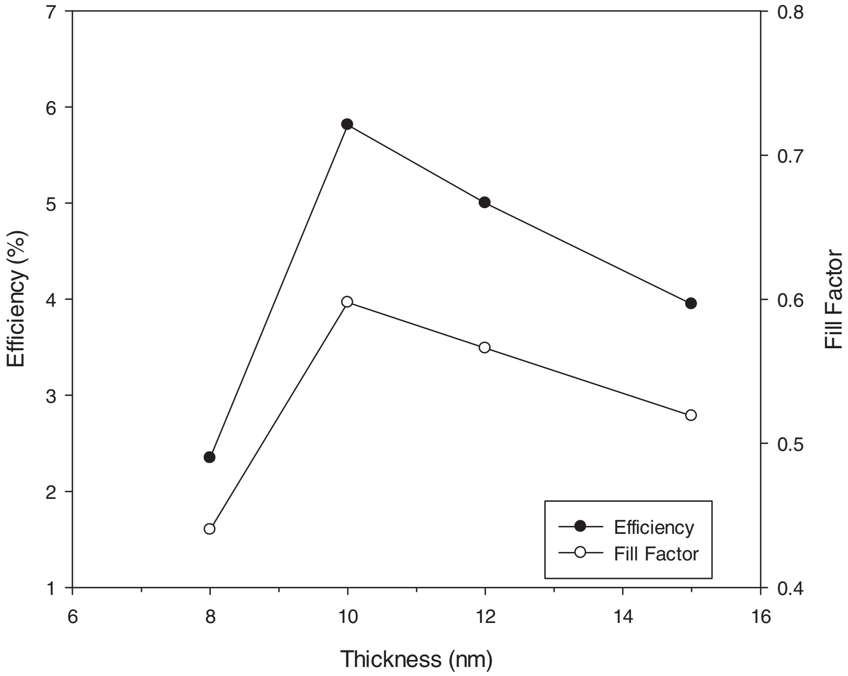

Figure 9. P-layer variation vs. efficiency and fill factor.

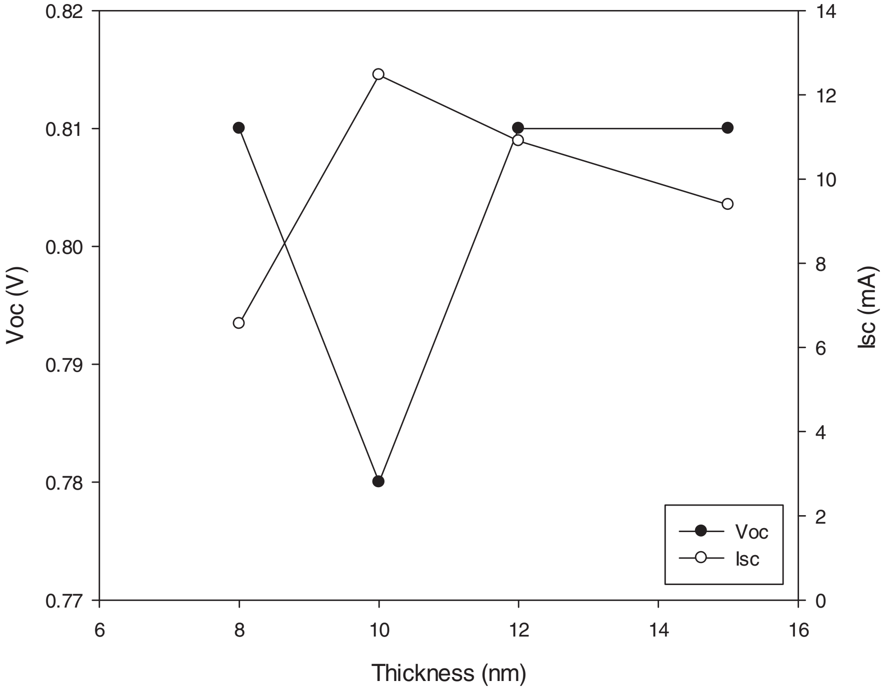

Figure 10. P-layer variation vs. V_{oc} and I_{sc}.

for this layer; if it is too thin then absorption will be reduced and I_{SC} will suffer, while if it is too wide then the electric field will be reduced causing impaired V_{OC}.

Contamination of the amorphous silicon material with impurities can also detrimentally affect the performance of this layer, resulting in significantly impaired I_{SC} values, regardless of other conditions. It is therefore essential that the deposition chamber is clean of all metal and other contamination, and dopant gases sufficiently cleared from the chamber using flows of inert gas after the doped layers. Parameters are shown as a function of intrinsic layer thickness, plotted against energy conversion efficiency, fill factor, V_{OC} and $I_{SC,}$ shown in Figs. 11 and 12, respectively. Layer thickness is varied from 360 nm to 390 nm in steps of 10 nm.

(3) Variation of n-Type Layer Thickness. The n-type layer thickness has less influence of the performance of the device compared to the other layers, as it is the final layer which the light will reach. In a similar way to the p-region, this layer only serves to create the electric field and does not contribute to carrier generation to any significant degree. It is however the layer which the unabsorbed light photons need to penetrate and be reflected from the rear contact reflector, to be absorbed within the intrinsic layer on their second pass.

In order to reduce recombination losses, the doping levels in this region are lower than in the p-type to help reduce the number of defects. Additionally, lower doping levels increase the silicon layer quality around the interface between intrinsic and amorphous material. The layer must therefore be wider in thickness in order to create an adequate electric field. Parameters are shown as a function of n-type layer thickness, plotted against

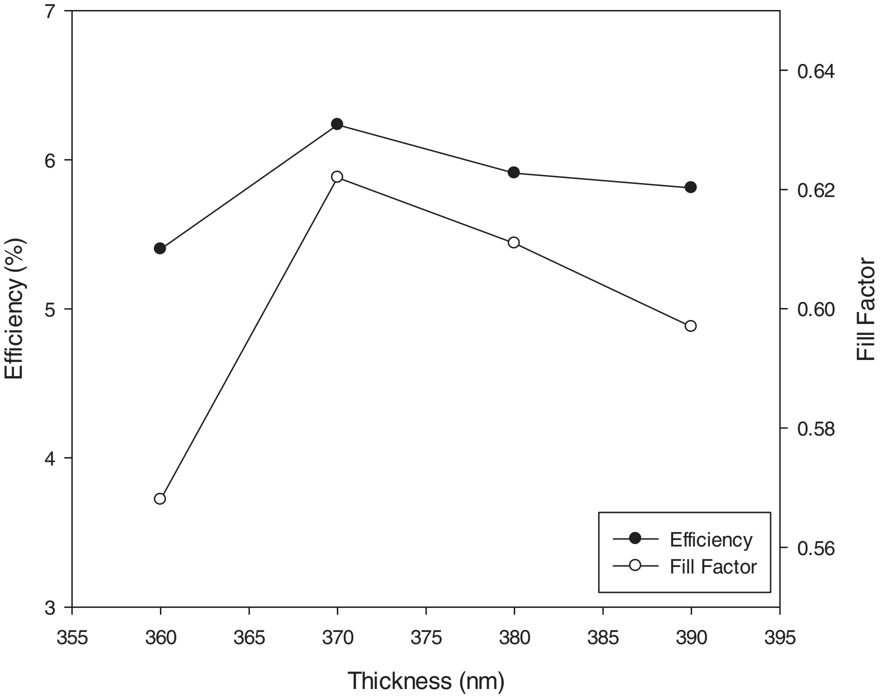

Figure 11. I-Layer variation vs. efficiency and fill factor.

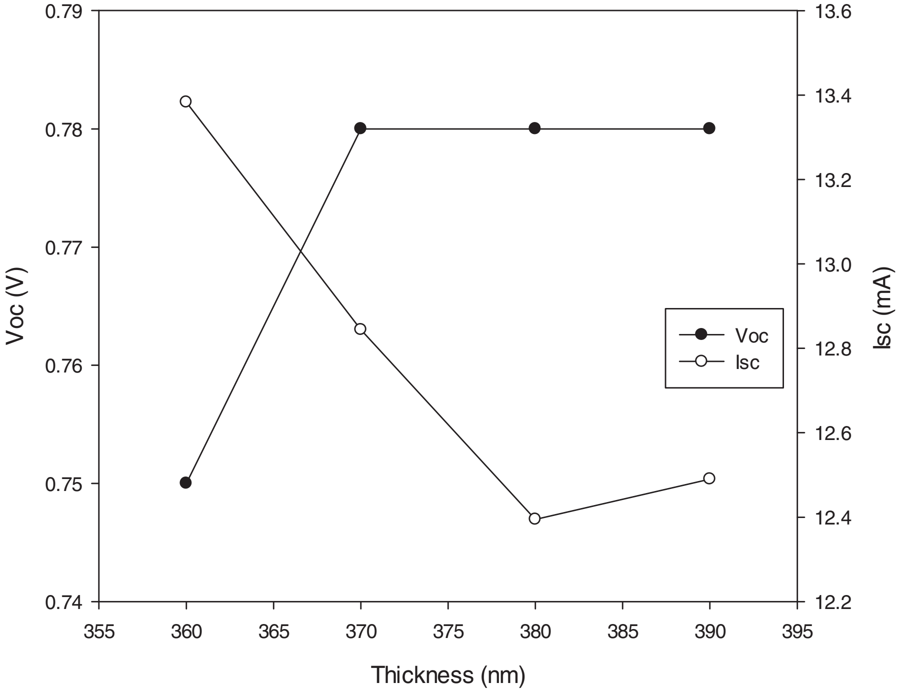

Figure 12. I-layer variation vs. V_{oc} and I_{oc}.

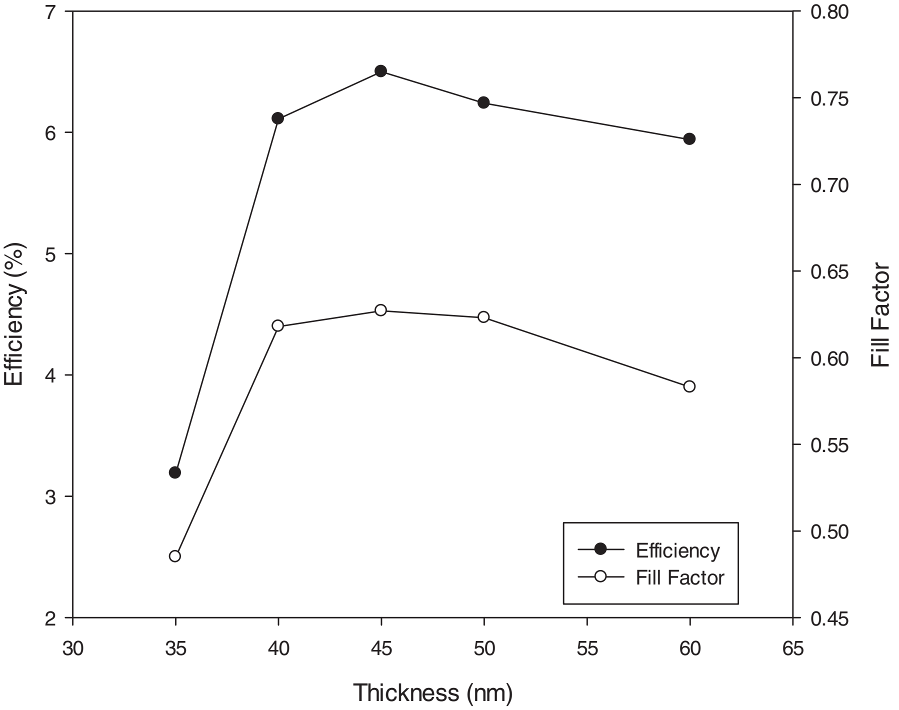

Figure 13. N-layer variation vs. efficiency and fill factor.

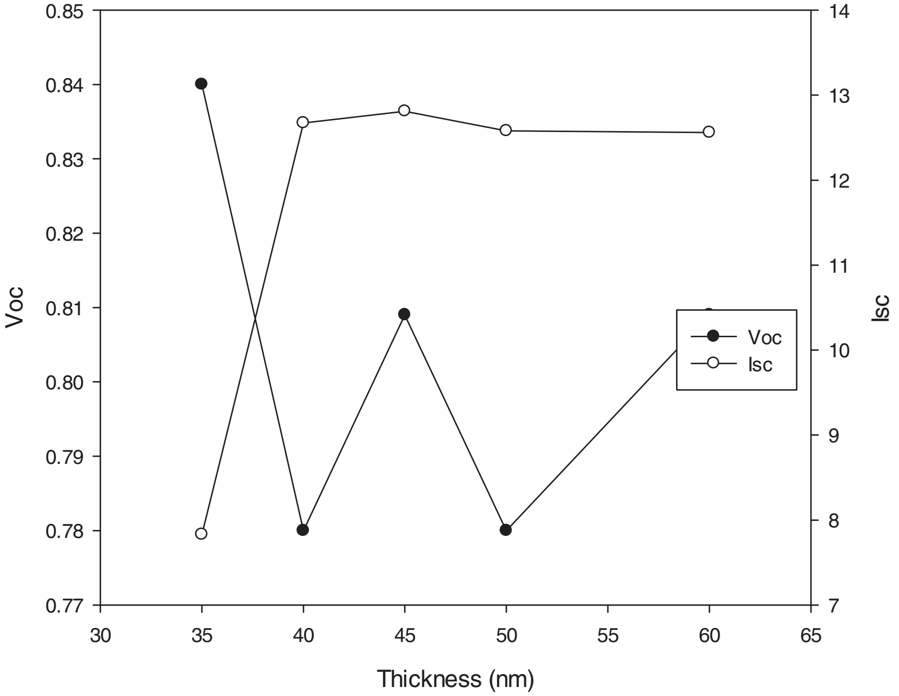

Figure 14. N-layer variation vs. V_{oc} and I_{sc}.

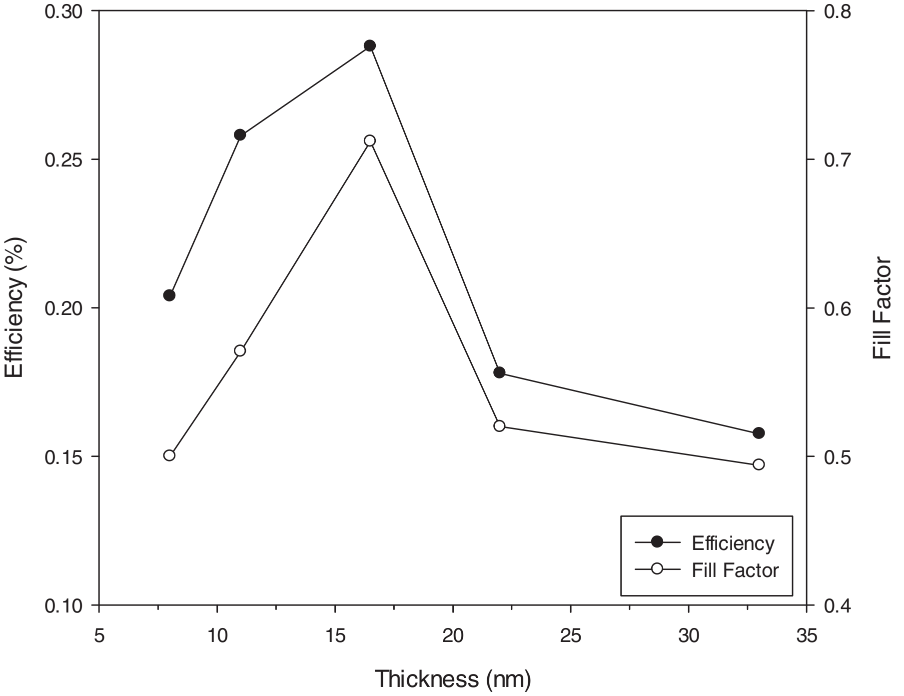

Figure 15. P-layer variation vs. efficiency and fill factor.

energy conversion efficiency, fill factor, V_{OC} and $I_{SC,}$ shown in Figs. 13 and 14, respectively. Layer thickness is varied from 30 nm to 60 nm in steps of 5 nm.

D. Use of Argon as a Dilute Gas

In order to realize high quality silicon films, it is essential to maintain accurate control over the deposition rate. In particular for p-type doped layers, the tolerance for the highest efficiency can be extremely thin. There is also the possibility of the plasma discharge taking ~1–2 sec to start at the beginning of the deposition at low pressures and power levels; this can lead to an ambiguous deposition time. It has previously been determined in Section A that mixing process gases with excess hydrogen results in reduced quality film, a possible solution to reduce deposition time is to mix the process gases with inert argon gas in the chamber. Due to the fact that the highest variation in performance is determined by variation of the p-layer thickness, this variable will be altered in a similar way to investigation C1, only with a high dilution of argon gas. Parameters are shown as a function of p-layer thickness, plotted against energy conversion efficiency, fill factor, V_{OC} and I_{SC}, shown in Figs. 15 and 16, respectively. Deposition conditions are presented in Table 3. Note that with high argon flow rates it is necessary to carry out depositions at a higher chamber pressure.

To further illustrate the effects of argon dilution, a selection of P-I-N devices are fabricated using the optimum conditions determined in the previous sections, with increasing flows or argon added to the process gas mixture.

Parameters are shown as a function of argon flow rate, plotted against energy conversion efficiency and fill factor of the measured P-I-N device, shown in Fig. 17. Argon flow rate is varied from 0 sccm to 500 sccm.

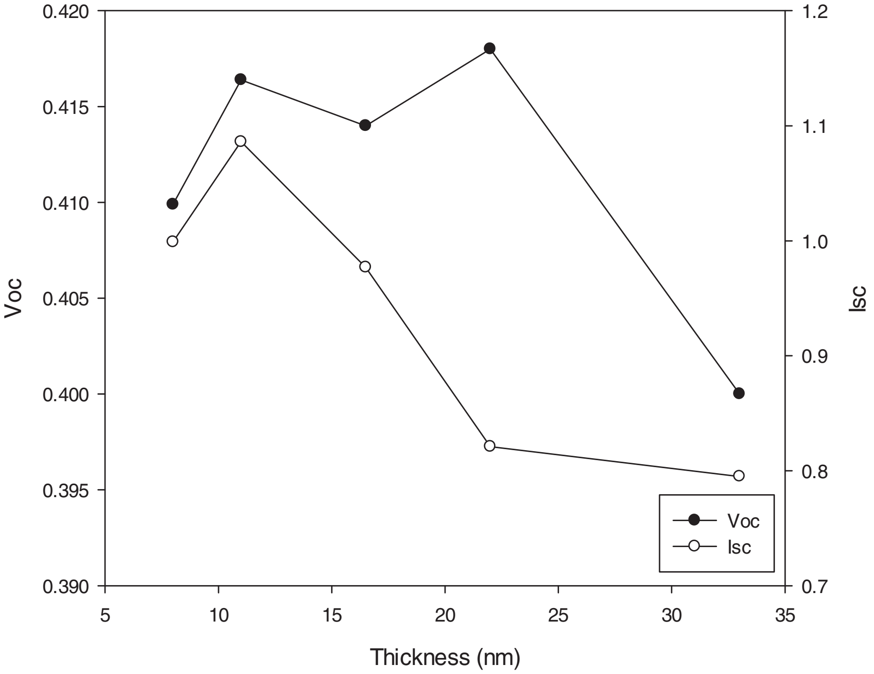

Figure 16. P-layer variation vs. *V*oc and *I*sc (Argon).

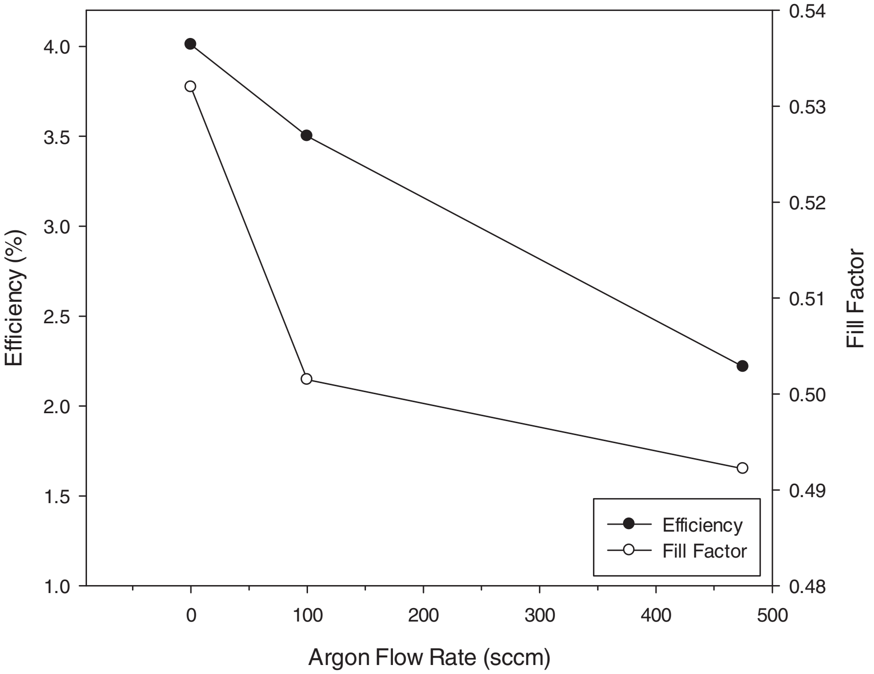

Figure 17. Argon flow rate variation.

V. Analysis

A. *Intrinsic Layer Results Summary*

Based on the results from investigation A, it is possible to determine under which conditions the optimum electrical properties from silicon material will be obtained.

From investigation 1, it can be observed that as the RF power is increased, the conductivity of the layer decreases and the dark/light ratio increases. While this is desirable, higher RF power (above 15 W) causes increased dust formation within the chamber, and as this dust becomes integrated into the film shunts are formed which reduce the number of active cells significantly. Additionally, higher RF power provides more kinetic energy to the species within the chamber, which will increase the deposition rate of the growing film. To ensure optimum yield, the RF power is kept at 10 W for all future depositions. Lower RF power additionally reduces ion bombardment damage caused to the growing films and can lead to higher quality material, however this can also reduce the number of weakly-bound hydrogen bonds within the silicon which would otherwise be broken by the plasma. This can result in a silicon film which is much more susceptible to the Staebler–Wronski effect after a period of light soaking [9].

Investigation 2 illustrates the effect of chamber pressure variations, which as can be seen exhibit a peak at 350 mT. Lower chamber pressures can cause problems stabilizing the RF plasma due to a reduction in airborne species while higher pressures increase the deposition rate to levels which are difficult to accurately control.

Investigation 3 shows the variation of substrate temperature, which can be seen to exhibit a large peak in photo-response at 250°C. The substrate temperature will also affect the deposition rate, which is easily controllable at 250°C but increases with temperature. Much higher temperatures can cause annealing of the amorphous material and microcrystalline formation which is undesirable for this investigation.

Investigation 4 presents four different dilutions of silane and hydrogen gas, which show that the optimum conditions are found with an equal 1:1 ratio of the two constituents.

Table 3. Argon layer deposition parameters

Variable	Unit	Value
RF power	(W)	10
Chamber pressure	(mTorr)	1000
Substrate temperature	(°C)	250
Gas flow rate (Silane)	(sccm)	50
Gas flow rate (Argon)	(sccm)	475
Gas flow rate (Diborane)	(sccm)	5
Gas flow rate (Phosphine)	(sccm)	2
Thickness	I (nm)	400
	N (nm)	55

Table 4. Intrinsic layer optimum conditions

Variable	Unit	Value
RF power	(W)	10
Chamber pressure	(mTorr)	350
Substrate temperature	(°C)	250
Gas flow rate (Silane)	(sccm)	50
Gas flow rate (Hydrogen)	(sccm)	50

Increasing the dilution past this level significantly reduces the deposition rate, and microcrystalline material is formed as ratios of 1:10 are approached which is demonstrated by a narrowing of the optical band gap from 1.7 eV toward 1.5 eV and lower. This is verified using Raman spectroscopy measurements. A 1:1 ratio of silane and hydrogen is therefore used for the optimum amorphous material.

A summary of the results from the intrinsic layer investigations are presented in the Table 4. These conditions are used within the P-I-N investigation in Section C. The contacting method of the single layers as prepared for measurement, with the four aluminum contract strips spaced 1 mm are shown in Fig. 18.

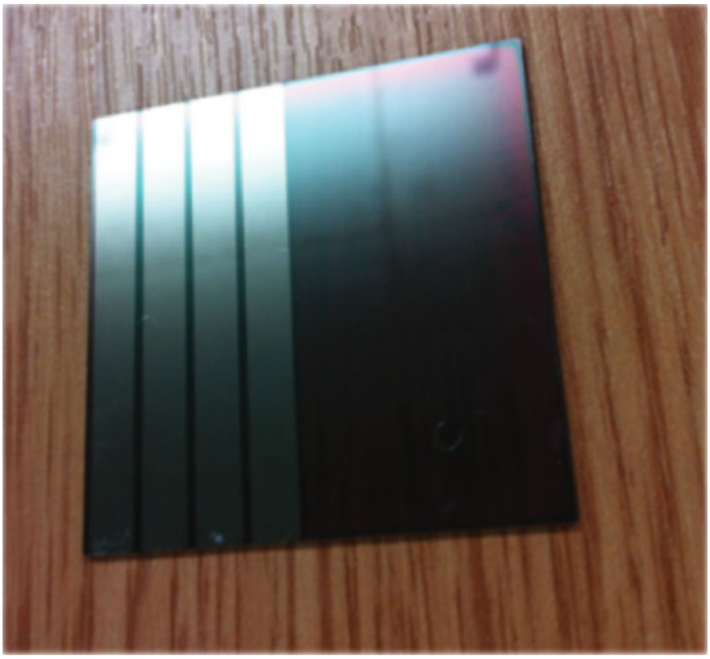

Figure 18. Thin film layer with 1 mm spaced contacts.

B. Doped Layer Results Summary

Based on the results from investigation B, it is possible to determine under which conditions the optimum electrical properties for the doped layers will be obtained.

From investigation 1, it can be observed that the silicon thin film begins doped-like behavior at concentrations exceeding 1%, with a peak in doped efficiency at around 2%. This corresponds to a diborane flow rate of 10 sccm. Due to the thickness requirement of this layer being so small, a high doping efficiency is essential for efficient charge carrier separation and therefore this flow rate is selected. Investigation 2 illustrates doped like behavior beginning at 0.5% and remaining fairly constant up to 2%. As this layer is able to be much thicker than the p-type region, a lower doping concentration can be chosen. To ensure reliable doping in all conditions but without creating excess recombination, a concentration of 1.2% is chosen which corresponds to a phosphine gas flow rate of 6 sccm.

A summary of the results from the doped layer investigation is presented in Table 5. These conditions are used within the P-I-N investigation in Section C. The same contacting method as used in investigation A is used for this set of measurements, as detailed in Fig. 18.

C. P-I-N Structure Results Summary

A summary of the results from the P-I-N thickness investigation is presented in Table 6. It can be observed that small variations in the p-type layer thickness result in the most profound variations in cell performance. The 10 nm appears to be the optimum point which maximizes cell performance, although a slight drop in I_{SC} is also observed which may be attributed to experimental error. The intrinsic region thicknesses vary over a much wider range, with 370 nm being the optimum. At this stage, it can be observed from the I_{SC} and V_{OC} charts that as the layer thickness is increased, the I_{SC} increases due to enhanced charge carrier collection but the V_{OC} decreases due to the influence of a weaker electric field across the region. The n-type layer shows a much less profound difference, with the 35 nm thickness showing a lower performance than the thicker devices of 40 nm and above. A figure illustrating the nine-region contacting method of the P-I-N layers, as prepared for measurement, is shown in Fig. 19. A full description of the effects of thickness variation is described in the analysis section.

Table 5. Doped layer optimum conditions

Variable	Unit	Value
Gas flow rate (Silane)	(sccm)	50
Gas flow rate (Hydrogen)	(sccm)	50
Gas flow rate (Diborane)	(sccm)	10
Gas flow rate (Phosphine)	(sccm)	6

Table 6. P-I-N device optimum conditions

Variable	Unit	Value
RF power	(W)	10
Chamber pressure	(mTorr)	350
Substrate temperature	(°C)	250
Gas flow rate (Silane)	(sccm)	50
Gas flow rate (Hydrogen)	(sccm)	50
Gas flow rate (Diborane)	(sccm)	10
Gas flow rate (Phosphine)	(sccm)	6
Optimum thickness	P (nm)	10
	I (nm)	375
	N (nm)	45
	Total (nm)	425
P-layer deposition time	(min:sec)	0:16
I-layer deposition time	(min:sec)	23:42
N-layer deposition time	(min:sec)	2:52
Deposition rate (P-layer)	(nm/sec)	0.60
Deposition rate (I/N-layer)	(nm/sec)	0.26

D. Use of Argon as a Dilute Gas

Results show that the use of argon gas as a dilution additive to the process gases has a detrimental effect to the device performance, reducing all efficiency values to below 1% in investigation D (Figs. 15 and 16). This may be partially due to the additional chamber pressure which is necessary to deposit under these conditions, however, the high chamber pressure investigations in Section A were not seen to reduce the intrinsic layer performance to this extent. The second investigation performed under optimized conditions in investigation D (Fig. 17) also shows a significant decrease in cell performance and fill factor as the argon dilution is increased. It is thought that the effect of the addition of argon, while chemically inert, causes increased ion bombardment damage to the growing films, increasing the amorphous disorder and displacing hydrogen passivation atoms from the matrix. This therefore significantly reduces the electrical performance of the layer.

E. Highest Performing Cell

The I-V curve and quantum efficiency data for the highest performing cell in this investigation is presented in Figs. 20 and 21. From this data, it is possible to determine information

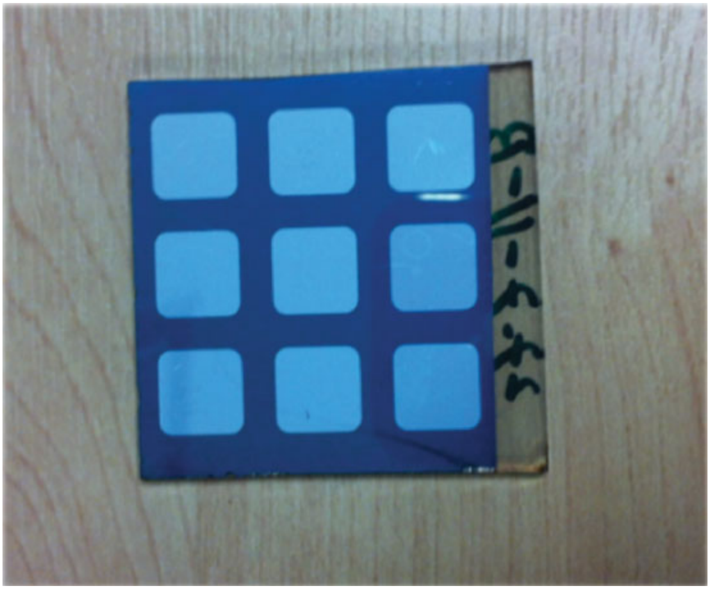

Figure 19. P-I-N device with 3 × 3 contact grid.

about the cell such as series resistance, shunt resistance, and maximum power point, which is detailed in the Table 7.

As can be observed, the device features a good V_{OC} and a strong I_{SC}, with a good fill factor leading to an excellent overall efficiency of 6.5%. The maximum power point is at 6.5 mW, which corresponds to a current of 10.84 mW and a voltage of 0.6 v. The quantum

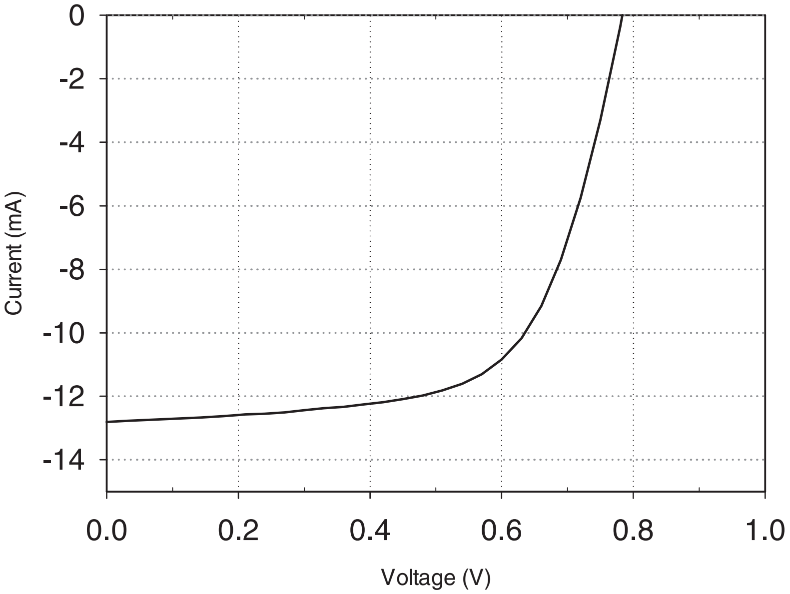

Figure 20. I-V curve of highest performance cell.

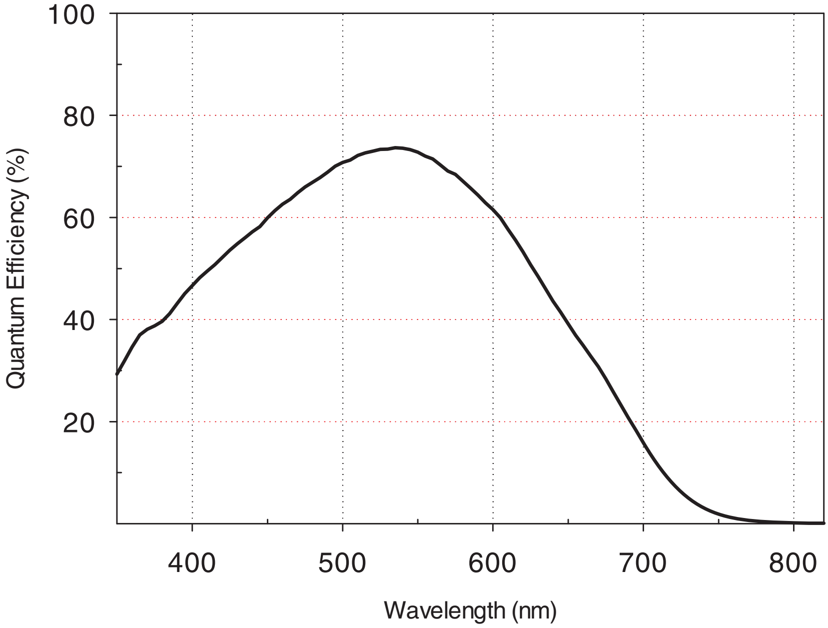

Figure 21. Quantum efficiency of highest performance cell.

efficiency shows high absorbtion in all regions expected of an amorphous silicon device, being particularly responsive to the blue and ultraviolet regions and a strong, even peak between 450 nm and 600 nm. Additionally, the R_{SH} value is adequately low which indicates an effective contacting method with minimal losses.

VI. Summary

Various deposition conditions have been used to demonstrate using an Oxford Instruments PlasmaLab System 100 to fabricate a-Si:H solar cells, and the optimum set of conditions has been identified. The effects of the variation of these conditions has been analyzed and explained, which can help diagnose problems with the deposition process. It was found that

Table 7. Measured characteristics of P-I-N device

Variable	Unit	Value
V_{OC}	(V)	0.81
I_{SC}	(mA)	12.81
V_{MP}	(V)	0.60
I_{MP}	(mA)	10.84
Max Power	(mW)	6.50
Fill Factor	—	0.63
Efficiency	(%)	6.50
R_S	(Ω)	19.3
R_{SH}	(Ω)	305

the maximum energy conversion efficiency possible using this system configuration was 6.5%, while improvement to this figure should easily be possible with the use of surface processing, light-trapping and antireflection technologies [10].

VII. Discussion

The investigation of the optimum quality of intrinsic and doped silicon material can be utilized in the planning and fabrication of more advanced solar cell structures, such as heterojunction (H-I-T) cells [11] and micro-morph [12] devices. The heterojunction design features an n-type single crystal silicon wafer which is passivated either side by nm-scale intrinsic amorphous silicon, creating a reduction in surface recombination velocity compared to conventional devices. This is due to the ∼5 nm "incubation layer" which forms on the surface of the substrate with poor electrical qualities and a high volume of SiH_2 bonds, thought to be due to the island growth formation of the amorphous silicon. This avoids the defect-rich doped layer from being deposited directly on the silicon surface, which would significantly increase recombination velocity [13]. The p-type emitter and an n-type back-surface field are then deposited on this intrinsic layer, which provide the p-n junction for charge carrier separation. It is therefore essential that this doped region is as effective as possible due to its very narrow thickness. Finally, layers of conductive TCO material are deposited to assist carrier collection between the contact regions. The micro-morph tandem design features a microcrystalline silicon and amorphous silicon heterojunction, which serves to combine the best of both technologies within the same device. The advantages of the tandem structure are primarily the broadening of the cell's absorption spectrum, which encompasses both regions of the a-Si and μc-Si junctions. The wide band-gap a-Si layer, which is positioned on the top surface of the structure, collects the high-energy blue and ultra-violet photons which would otherwise not be absorbed by a microcrystalline cell alone. The uncollected photons then pass through the microcrystalline region that is sensitive to the lower energy red and infra-red photons.

Acknowledgment

This work was supported in part by the Engineering and Physical Sciences Research Council.

References

[1] SolarBuzz, *Thin Film Module Supply*, Available at: http://www.solarbuzz.com/reports/.

[2] Spear, W. E., Le Comber, P. G., Kinmond, S., & Brodsky, M. H. (1976). *Appl. Phys. Lett.*, *105*, 28.

[3] Carlson, D. E., & Wronski, C. R. (1976). *Appl. Phys. Lett.*, *28*(11), 671.

[4] Poortmans, J., & Arkhipov, V. (2006). *Thin Film Solar Cells: Fabrication, Characterization and Applications*, Wiley: Chichester, UK, p 205.

[5] Pilkington NSG TEC (Technical Applications) (2012). *Global Glass Handbook*, Pilkington Group Ltd.: St. Helens, UK.

[6] Shockley, W., & Read, W. T., Jr. (1952). Statistics of the recombinations of holes and electrons. *Phys. Rev.*, *87*, 835.

[7] Spear, W. E., & Le Comber, P. G. (1975). Substitutional doping of amorphous silicon. *Solid State Commun.*, *17*(9), 1193–1196.

[8] Ito, T., Imaizumi, M., Konomi, I., & Yamaguchi, M. (1997). Effect of hydrogen content on the crystalline quality of PECVD-deposited silicon for solar cells. In: *Photovoltaic Specialists Conference, Conference Record of the Twenty-Sixth IEEE*, Anaheim, CA, 747–750.

[9] Mahan, A. H., Carapella, J., Nelson, B. P., Crandall, R. S., & Balberg, I. (1991). *J. Appl. Phys.*, *69*, 6728.

[10] Deckman, H. W., Wronski, C. R., Witzke, H., & Yablonovitch, E. (1983). Optically enhanced amorphous silicon solar cells. *Appl. Phys. Lett.*, *42*(11), 968.

[11] Tanaka, M., Taguchi, M., Matsuyama, T., Sawada, T., Tsuda, S., Nakano, S., Hanafusa, H., & Kuwano, Y. (1992). *Jpn. J. Appl. Phys.*, *31*, 3518.

[12] Meier, J., Spitznagel, J., Kroll, U., Bucher, C., Fay, S., Moriarty, T., & Shah, A. (2003). In: *Proceedings of 3rd World Conference*, Osaka, Japan, pp. 2801–2805, Vol. 3 (18 May 2003).

[13] Kondo, M., De Wolf, S., & Fujiwara, H. (2008). *MRS Proceedings* (Vol. 1066, No. 1). Cambridge University Press: Cambridge, UK.